Progress Energy

John W. Moyer
Vice President
Robinson Nuclear Plant
Progress Energy Carolinas, Inc.

Serial: RNP-RA/03-0141

NOV 2 1 2003

Mr. James E. Dyer
Director, Office of Nuclear Reactor Regulation
United States Nuclear Regulatory Commission
Washington, DC 20555-0001

H. B. ROBINSON STEAM ELECTRIC PLANT, UNIT NO. 2
DOCKET NO. 50-261/LICENSE NO. DPR-23

SUPPLEMENT TO THE REQUEST FOR RELAXATION FROM THE ORDER FOR ESTABLISHING INTERIM INSPECTION REQUIREMENTS FOR REACTOR PRESSURE VESSEL HEADS AT PRESSURIZED WATER REACTORS (EA-03-009)

Dear Mr. Dyer:

By letter dated August 15, 2003, Progress Energy Carolinas, Inc. (PEC), provided a request for relaxation of the subject Order in accordance with the provision of the Order that states the Director, Office of Nuclear Reactor Regulation, may, in writing, relax or rescind any of the conditions of the Order upon demonstration by the licensee of good cause.

In meetings between your staff and personnel representing H. B. Robinson Steam Electric Plant (HBRSEP), Unit No. 2, on September 25 and October 16, 2003, it was determined that additional information would assist in their review. That information is provided by this letter.

Also, in discussions with your staff we have been requested to provide a desired schedule for completion of the NRC review of this request. Some of the factors that are relevant to the timely review of the proposed relaxation include the methods of examination that will be required and the scope of the examinations. The next refueling outage for HBRSEP, Unit No. 2, is scheduled to begin in April 2004. Therefore, completion of the NRC review by December 31, 2003, is respectfully requested.

The information contained in this letter, attachment, and enclosure is true and correct to the best of my information, knowledge, and belief; and the sources of my information are officers, employees, contractors, and agents of PEC. I declare under penalty of perjury that the foregoing is true and correct.

If you have any questions concerning this matter, please contact Mr. C. T. Baucom.

Sincerely,

J W Moyer

John W. Moyer

3581 West Entrance Road
Hartsville, SC 29550

A101

CTB/cac

Attachment

Enclosures

c: Mr. L. A. Reyes, NRC, Region II
Mr. C. P. Patel, NRC, NRR
NRC Resident Inspector
NRC Document Control Desk

H. B. ROBINSON STEAM ELECTRIC PLANT, UNIT NO. 2

ADDITIONAL INFORMATION FOR THE REQUEST FOR RELAXATION FROM THE ORDER REQUIREMENTS FOR REACTOR PRESSURE VESSEL HEADS AT PRESSURIZED WATER REACTORS (EA-03-009)

In meetings with the NRC staff on September 25 and October 16, 2003, it was determined that additional information would assist in the review of the proposed request for relaxation from the Order requirements for the H. B. Robinson Steam Electric Plant (HBRSEP), Unit No. 2, reactor pressure vessel (RPV) head. The additional information is provided as follows:

Additional Description of Parent Tube Indications

The ultrasonic examination results from the fall 2002 refueling outage for HBRSEP, Unit No. 2, showed seven (7) RPV head penetrations had indications that were recorded as "parent tube indications" (PTI). Additionally, two (2) penetrations were listed with "weld interface indications" (WII), which are very similar to the PTIs. After further review and analysis, it has been determined that the PTIs and WIIs would no longer be considered recordable. These indications were subjected to additional detailed analysis to determine the nature of the indications; in particular, to differentiate between primary water stress corrosion cracking (PWSCC)-type signals and metallurgical reflectors. In each case, the PTIs and WIIs were confirmed to be metallurgical reflectors associated with the weld-to-base metal interface, and not PWSCC. The data sheets document this additional analysis, and the final analysis conclusion was "no detectable defect" (NDD). Therefore, there were no recordable ultrasonic indications.

A review of the PTIs for HBRSEP, Unit No. 2, concluded that in each case the signal was determined to be a geometric reflector and was not indicative of a crack-type indication. During the fabrication of the HBRSEP, Unit No. 2, RPV head, grinding for interim penetrant testing was typically done three times: (1) after the root pass, (2) after approximately mid-weld, and (3) after the final pass. In these locations, a geometric reflector can be introduced due to the grinding and subsequent weld pass interface. Using more recent data analysis guidelines, these signals would no longer be recorded as PTI.

Lateral Wave Detection Limits

The type of open housing scanner (Westinghouse 7010) used in the HBRSEP, Unit No. 2, ultrasonic (UT) and eddy current (ET) examination of seventeen (17) open housing penetrations was also used in a CRDM/MRP/EPRI demonstration during September 2002 for detection and sizing. In this demonstration, eddy current testing was used for inner surface detection and length sizing. Therefore, during this phase of the demonstration, no specified minimum detection size was formally demonstrated for the UT, however, flaws were depth-sized down to 0.8 mm (0.031 inch).

Although not conducted as part of the formal demonstration, tests of scanning methods at another facility in April 2002 showed that by scanning manually with the PCS24 open tube probe (the same type of probe used for HBRSEP, Unit No. 2), inner surface connected flaws in the range of 1.5 mm (0.059 inches) to 8.0 mm (0.314 inches) could be detected by a break in the lateral wave.

Nine (9) out of the seventeen (17) open tube housing examinations had indications of craze cracking as detected by ET. This phenomenon was typically found at the 180 degree location below the weld. The craze cracking was not detectable with time-of-flight-diffraction (TOFD) UT probes, indicating that depths were less than 0.040 inches.

Eddy current testing of the inner surface on the fifty-two (52) thermally sleeved penetrations was conducted using the Gapscanner. Seven (7) of these penetrations showed evidence of craze cracking. These indications had eddy current characteristics similar to those identified with the open housing scanner in terms of low amplitude and small phase angle.

Further confirmation of the typical depth and detection of craze cracking was found during inspections conducted at Millstone Unit 2 and documented in an ABB/CE report in January 1998. Nozzle 15 had eddy current indication of craze cracking that was also confirmed by fluorescent penetrant testing. A cluster of 22 shallow crack indications was detected. Through comparison with the ultrasonic TOFD method lateral wave response, the depth estimate was less than 0.022 inches from the inner diameter surface. Sequential grinding was performed with intermediate eddy current testing. After the flaws were no longer detectable, an additional flapper wheel grinding step was performed to eliminate flaws that may have been less than the ET detection limit. A final ET and fluorescent penetrant test were performed and confirmed that the metal removal was 0.032 inches.

The analyses performed for flaw propagation for HBRSEP, Unit No. 2, submitted with the August 15, 2003 letter, which conservatively include initial flaws of greater depth than craze cracking, conclude that such flaws are not expected to propagate through the reactor coolant pressure boundary during the requested period of deferral.

<u>Recent Experience at Millstone Unit 2</u>

In the information provided by the HBRSEP, Unit No. 2, letter dated August 15, 2003, it was shown that only one operating unit with similar RPV head characteristics (i.e., Combustion Engineering-manufacture with Huntington alloy tubes) had shown evidence of degradation. During inspections conducted in February 2002 at Millstone Unit 2, three (3) penetration tubes were found with indications that appeared to have originated at the outer diameter surface and propagated towards the J-groove weld. The flaws also appeared to remain predominantly in the tube material and did not significantly propagate into the weld. No evidence of leakage was found from these penetrations.

In recent examinations conducted at Millstone Unit 2 in October 2003, eleven (11) additional tubes have been found with flaws similar to those discovered in 2002. Further evaluation of this condition has been conducted for HBRSEP, Unit No. 2. This evaluation included the following considerations:

- The worst case uninspected area was 0.125 inches below the bottom of the weld. Therefore, flaws were postulated with the upper extremity at 0.125 inches below the weld.
- The flaw location was postulated on the tube outer diameter.
- Aspect ratios of 3:1 and 6:1 were considered.
- Initial flaw depths of 10%, 20%, 50%, and 75% of the tube thickness were considered.
- The analysis method used for stress intensity factors was Raju and Newman.
- Growth was calculated based on K results at the upper extremity of the flaw.
- The crack growth model of MRP-55 was used.
- The flaw shape was assumed to remain constant.

The results of this evaluation are provided graphically, as follows:

Results for outer diameter flaw, a/t = 0.1

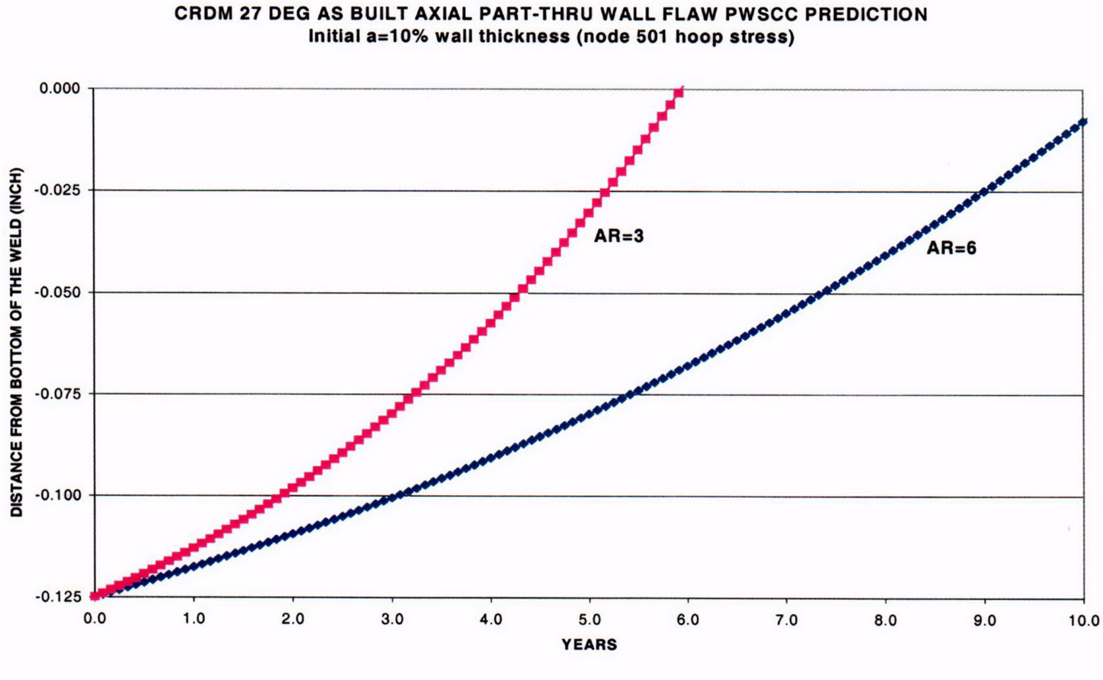

C-01

Results for outer diameter flaw, a/t = 0.2

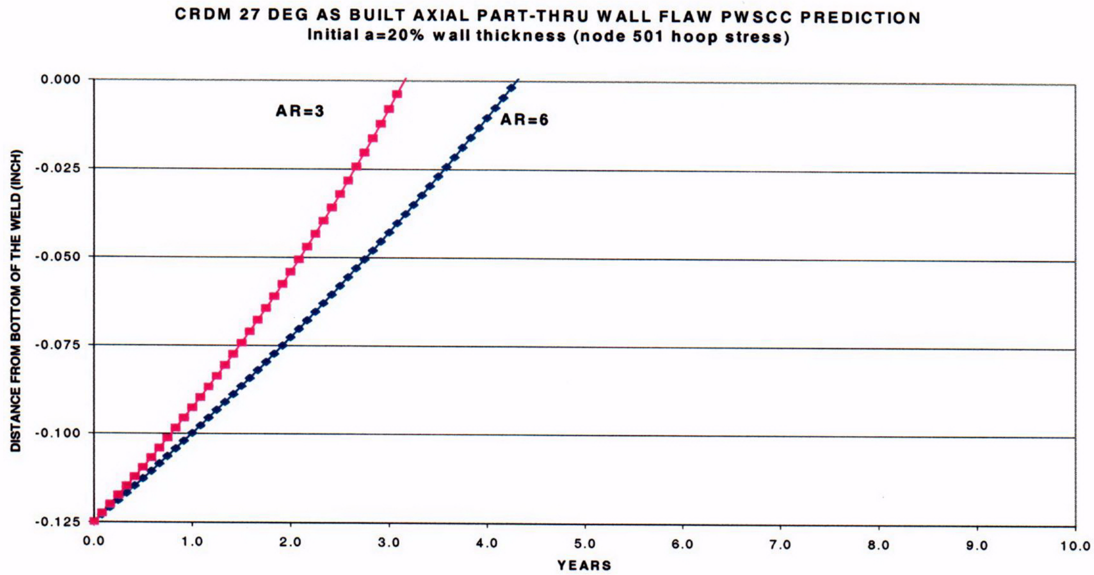

Results for outer diameter flaw, a/t = 0.5

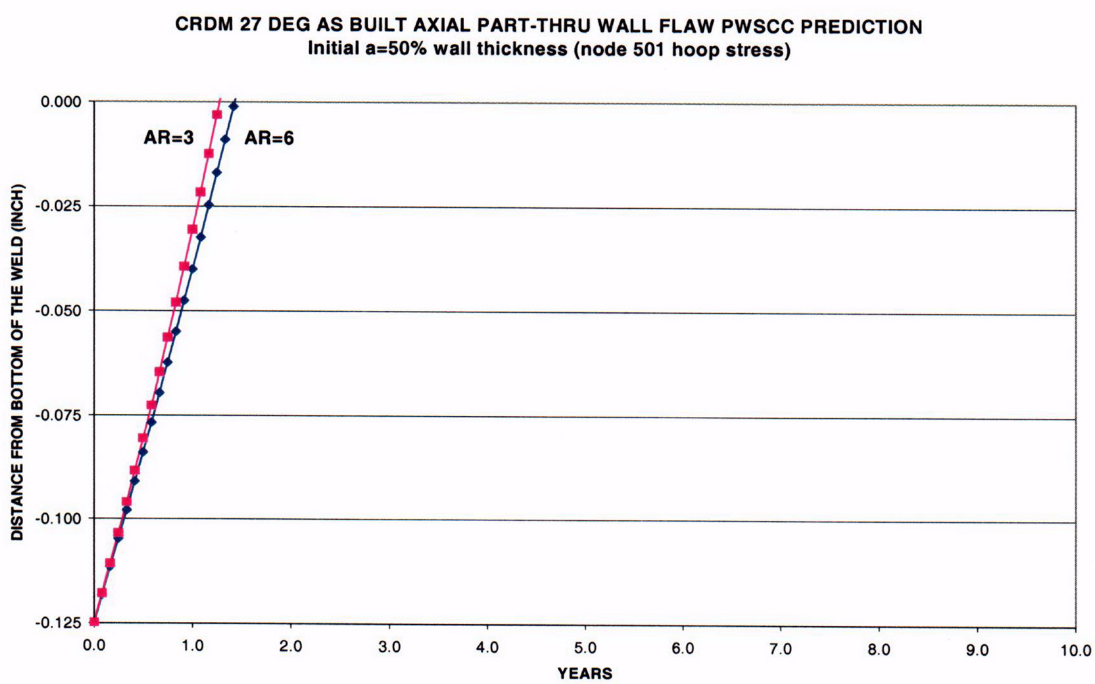

C-02

Results for outer diameter flaw, a/t = 0.75

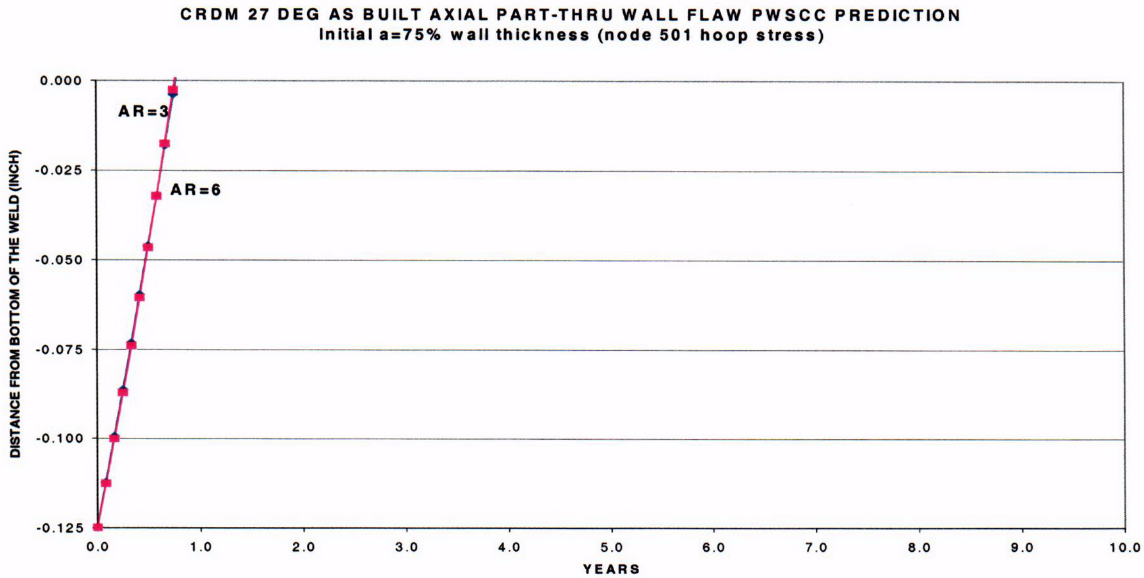

As demonstrated by these results, initial flaws with greater percentages of through-wall result in less time to reaching the bottom of the weld. After reaching the bottom of the weld, propagation through the weld is dependent on location (weld thickness) and weld crack growth predictions (see DEI Report R-3515-00-1, "Technical Basis for RPV Head CRDM Nozzle Inspection Interval H. B. Robinson Steam Electric Plant, Unit No. 2," Revision 0, July 2003).

Additionally, DEI completed an informal calculation of weld crack growth assuming an initial depth of 0.16 inches (4 mm), which resulted in an estimated 1.6 years to grow from the bottom of the as-built weld to the annulus at the top of the weld (approximately 1.8 inches for a 27 degree nozzle). By using the Westinghouse tube crack growth graphical information, it can be concluded that, using these assumptions, crack propagation from the uninspected region of the tube through the pressure boundary would take greater than three years based on an undetected flaw not exceeding approximately 40% through-wall on the outer diameter of the tube.

Review of tube material data revealed that the heat number for the Millstone Unit 2 penetration tubes is different than the heat numbers for the HBRSEP, Unit No. 2, penetrations. HBRSEP, Unit No. 2, shares RPV head penetration tube heat numbers with Connecticut Yankee, Diablo Canyon 1, Indian Point 2, and Salem 1. The discovery of degradation at Millstone Unit 2 appears to further support the postulation that factors other than time and temperature may affect susceptibility to primary water stress corrosion cracking.

Additional Analysis of Through-Wall Circumferential Cracking

Material supplementing DEI Report R-3515-00-1, Revision 0, and the supporting DEI calculation C-3515-00-4, are provided as enclosures to this letter.

DEI Stress Intensity Factor Calculation for Through-Wall Circumferential Cracks in the Outer Row Robinson CRDM Nozzle

Material Supplementing DEI Report R-3515-00-1, Rev. 0,
and Supporting the September 25, 2003,
Meeting Between Progress Energy and the NRC Staff
to Discuss the Progress Energy Request for Relaxation
from the Requirements of NRC Order EA-03-009

Dominion Engineering, Inc.
Nonproprietary

Glenn White
Steve Hunt
John Broussard
David Gross

Overview

- Purpose
- Calculation Methodology
- Robinson Results
- Comparison with Other Stress Intensity Factor (SIF) Curves
- Model Verification and Validation Test Cases
- Effect on Nozzle Ejection Assessments in DEI Report R-3515-00-1, Rev. 0
  - Deterministic Results
  - Probabilistic Results

Purpose

- The calculations of circumferential crack growth documented in DEI Report R-3515-00-1, Rev. 0, are based on a stress intensity factor calculation performed by the Materials Reliability Program (MRP):
  - Based on a Westinghouse plant design with very similar nozzle and weld dimensions to Robinson
  - Presented to the NRC staff on June 12, 2003
  - Documented in Report MRP-95 (Plant C)
- Work performed in parallel to Report R-3515-00-1, Rev. 0, to calculate Robinson-specific stress intensity factors using a DEI fracture mechanics FEA model is now complete
- This presentation summarizes the new calculation and its effect on the nozzle ejection risk assessments of R-3515-00-1, Rev. 0

Calculation Methodology
Summary

- The calculation methodology and detailed results are provided in DEI Calculation C-3515-00-4, Rev. 0 (Nonproprietary)
- Through-wall crack in outer row (46.0°) CRDM nozzle parallel to weld contour with variable distance above top of weld and bounding nozzle yield strength of 53 ksi
- Custom fracture mechanics code added to DEI welding residual finite-element stress model for J-groove nozzles
- Stress redistribution from intact to cracked conditions modeled
  - Redistribution modeled as an elastic unloading problem amenable to LEFM
- Equivalent stress intensity factor (*K*) calculated from J-integral
  - J-integral calculated using numerical volume integration
  - J-integral averaged across nozzle wall
  - J-integral approach captures effect of Mode II and III contributions

$$K_{eq} = \sqrt{\frac{J_{avg}E}{1-\nu^2}}$$

Calculation Methodology
Fracture Mechanics FEA Model for Robinson

180° Downhill-Centered Crack

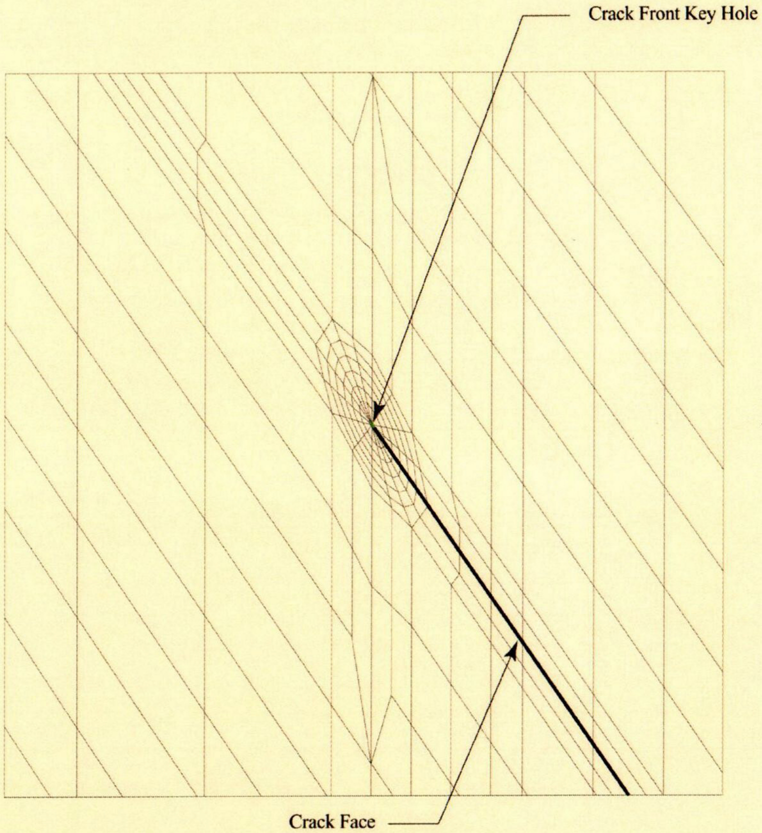

Crack Mesh Detail

C-04

Robinson Results
Downhill-Centered Cracks

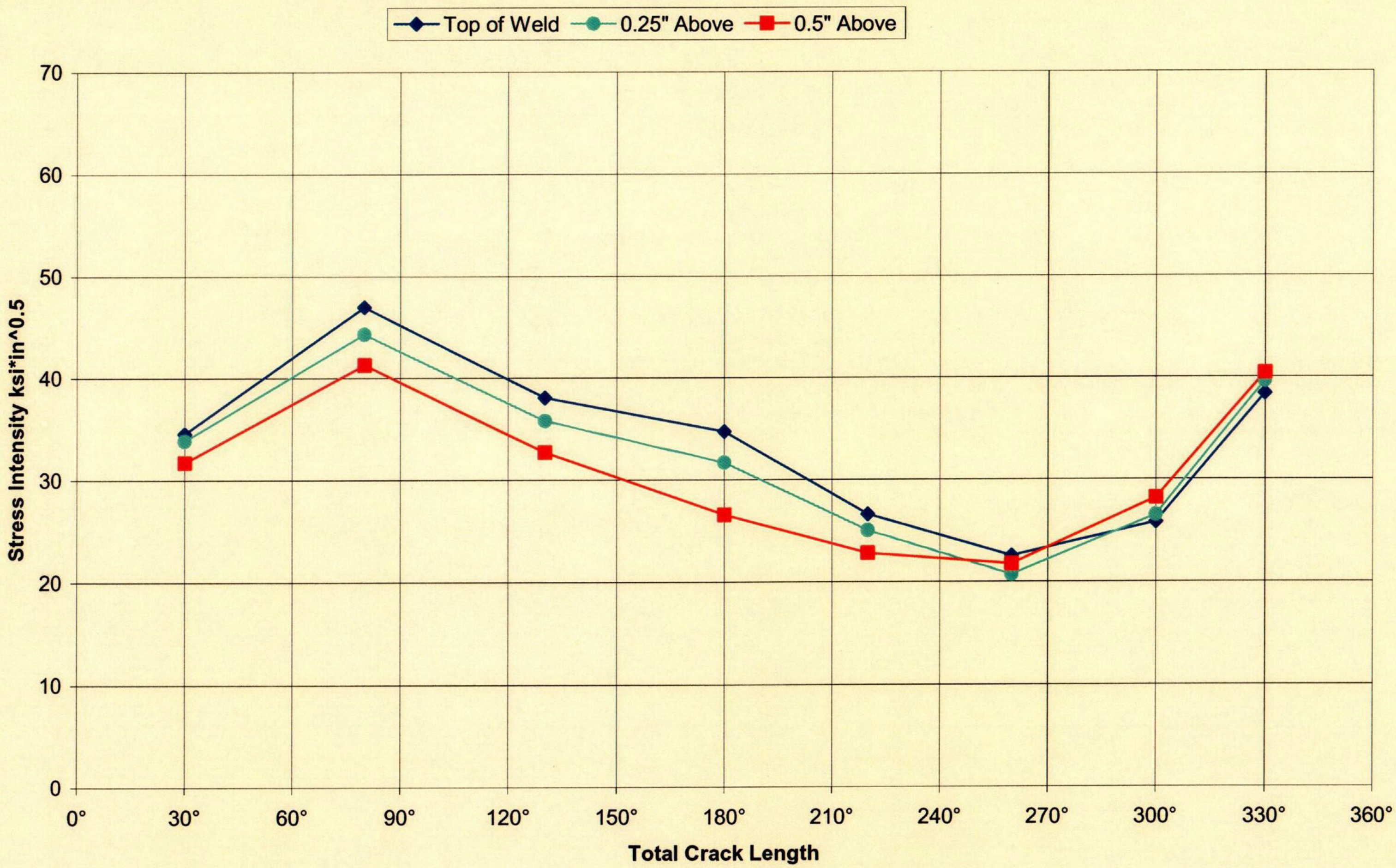

C-05

Robinson Results
Uphill-Centered Cracks

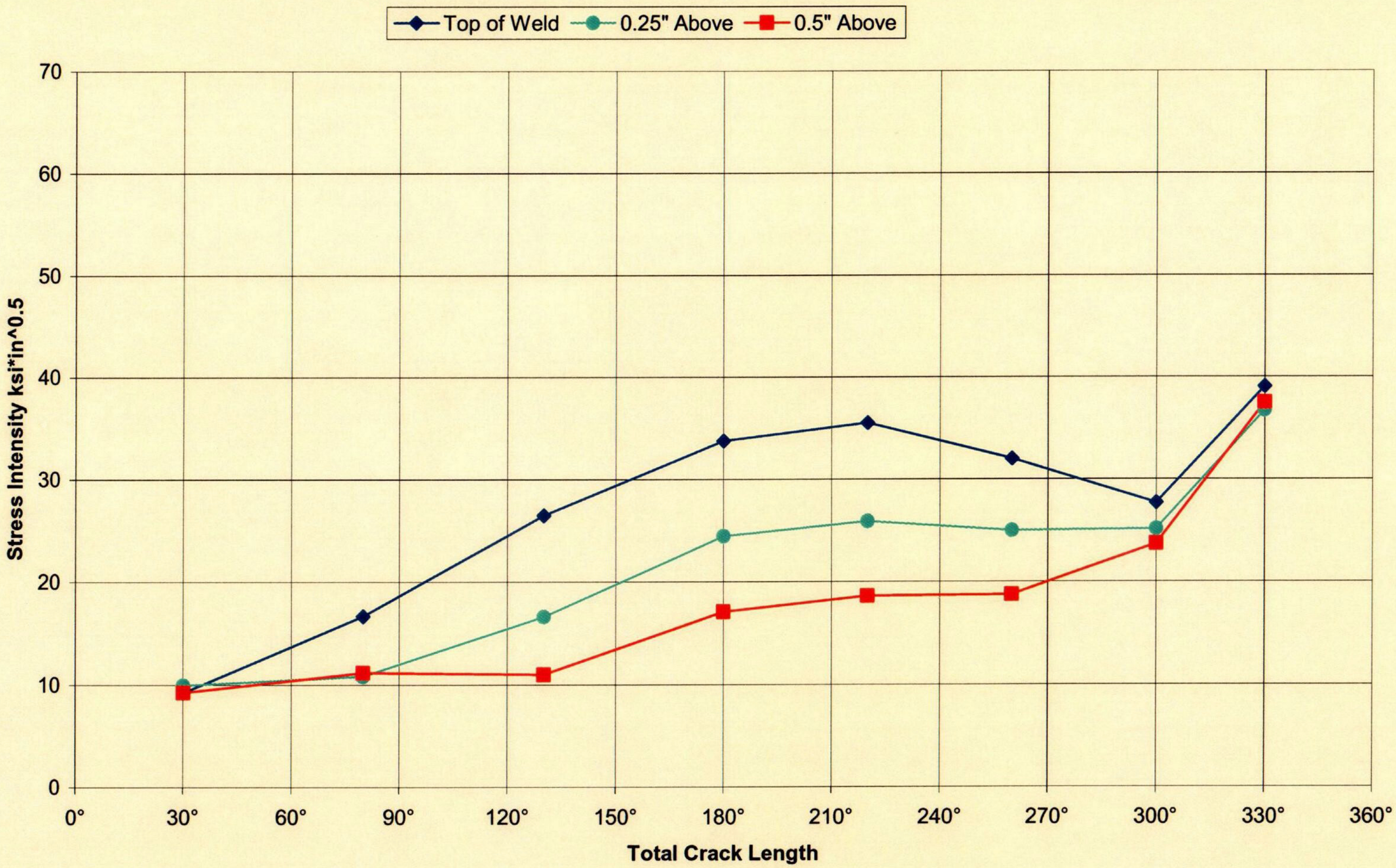

C-96

Comparison with Other SIF Curves
Downhill-Centered Cracks

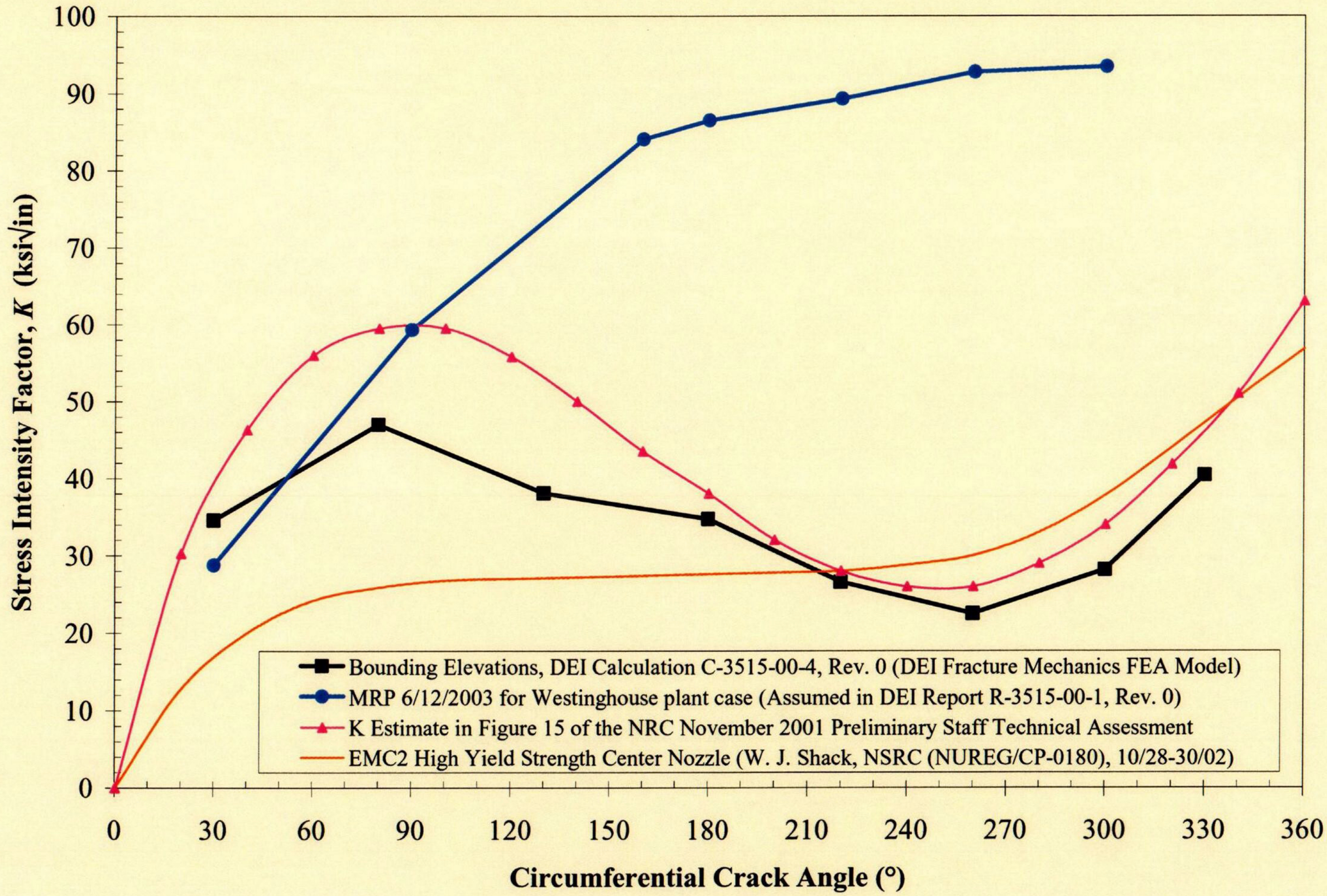

C-07

Comparison with Other SIF Curves
Uphill-Centered Cracks

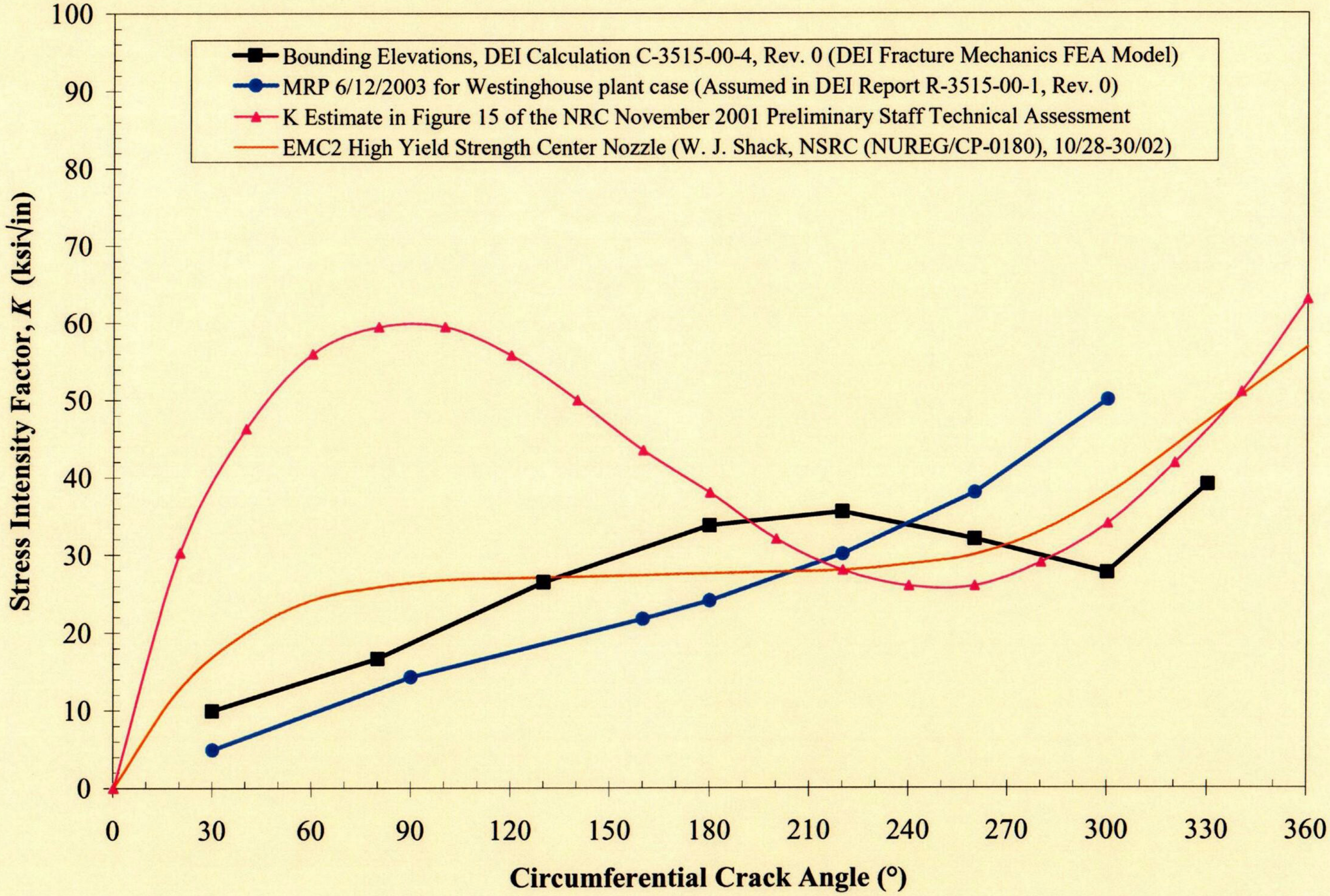

C-08

Model Verification and Validation Test Cases
Pipe Loaded Under Axial Tension

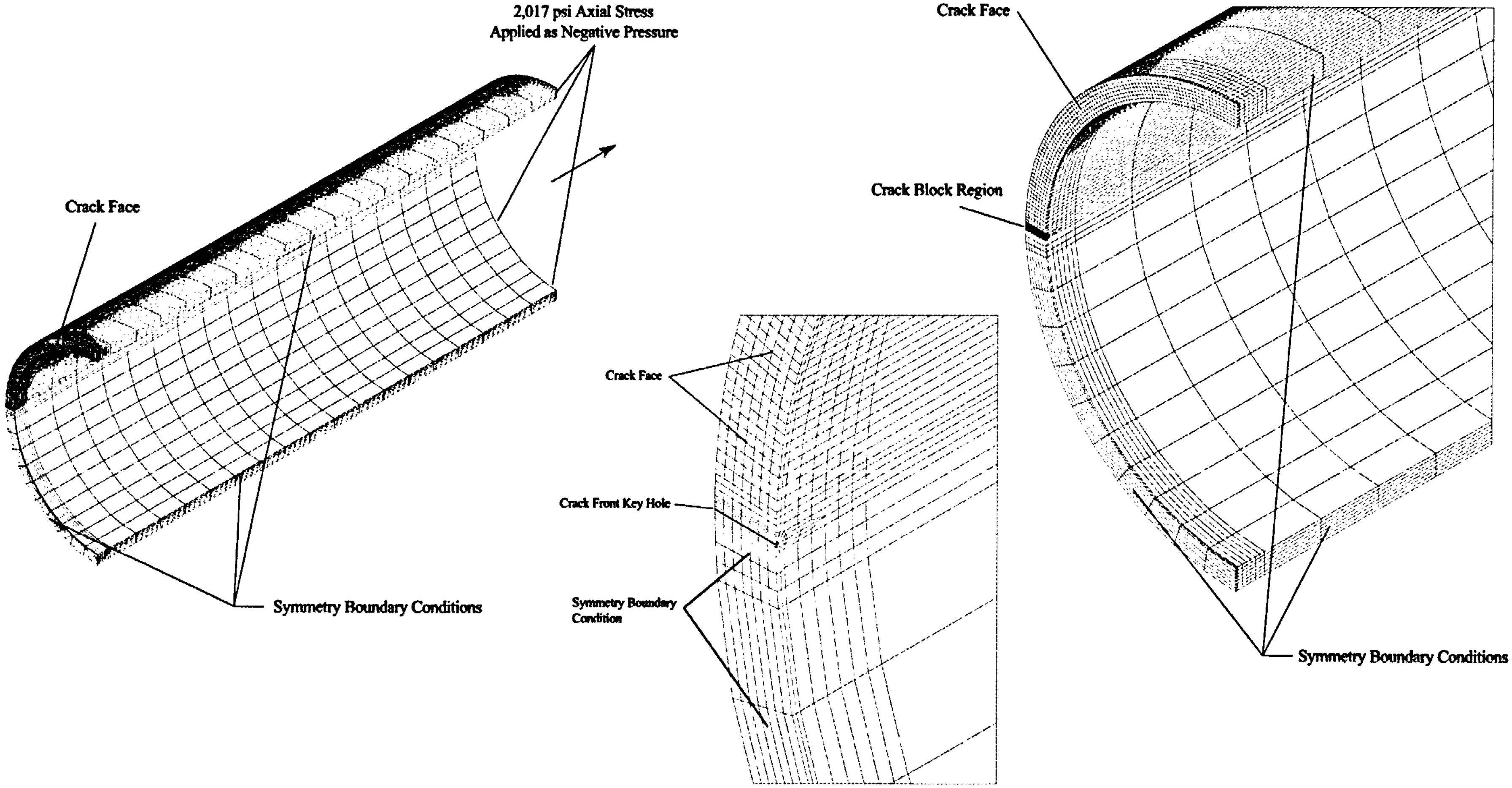

Model Verification and Validation Test Cases
Pipe Loaded Under Axial Tension (cont'd)

- As part of the model verification and validation, a model of a pipe with a through-wall circumferential flaw and subject to axial tension was created
- The stress intensity factor calculated for this model was compared to the results published by Zahoor[1] for a mean radius to wall thickness ratio of 10 and a maximum total crack arc of 180°:

Crack Length	K_I Calculated Using Zahoor[1]	K Calculated per FEA Model Test Case
30°	2.9 ksi$\sqrt{\text{in}}$	2.9 ksi$\sqrt{\text{in}}$
80°	6.6 ksi$\sqrt{\text{in}}$	7.1 ksi$\sqrt{\text{in}}$
130°	12.7 ksi$\sqrt{\text{in}}$	13.6 ksi$\sqrt{\text{in}}$
180°	24.0 ksi$\sqrt{\text{in}}$	26.5 ksi$\sqrt{\text{in}}$

[1]A. Zahoor, ***Ductile Fracture Handbook*, *Volume 1*, EPRI, Palo Alto, CA: 1989. NP-6301-D.**

Model Verification and Validation Test Cases
Through-Wall Center Crack in Plate

- For large crack sizes, the residual stresses are mostly relieved and the pressure stress determines the stress intensity factor

- A published solution[2] for a through-wall crack in a finite plate for all *a*/*b* and large *h*/*b* was compared to the results for Robinson for large circumferential cracks
  - The remote axial stress σ was based on the axial pressure loading including pressure on the crack face

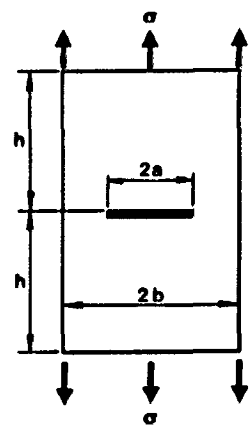

$$K_0 = \sigma\sqrt{\pi a}; \qquad \frac{K_I}{K_0} = \frac{1 - 0.5\frac{a}{b} + 0.326\left(\frac{a}{b}\right)^2}{\sqrt{1-\frac{a}{b}}}$$

Note: *a* is taken as the projection of the crack midwall half-length on a horizontal plane.

[2]**D. P. Rooke and D. J. Cartwright, *Compendium of Stress Intensity Factors*, Her Majesty's Stationery Office, London, 1976, p. 10.**

Model Verification and Validation Test Cases
Through-Wall Center Crack in Plate (cont'd)

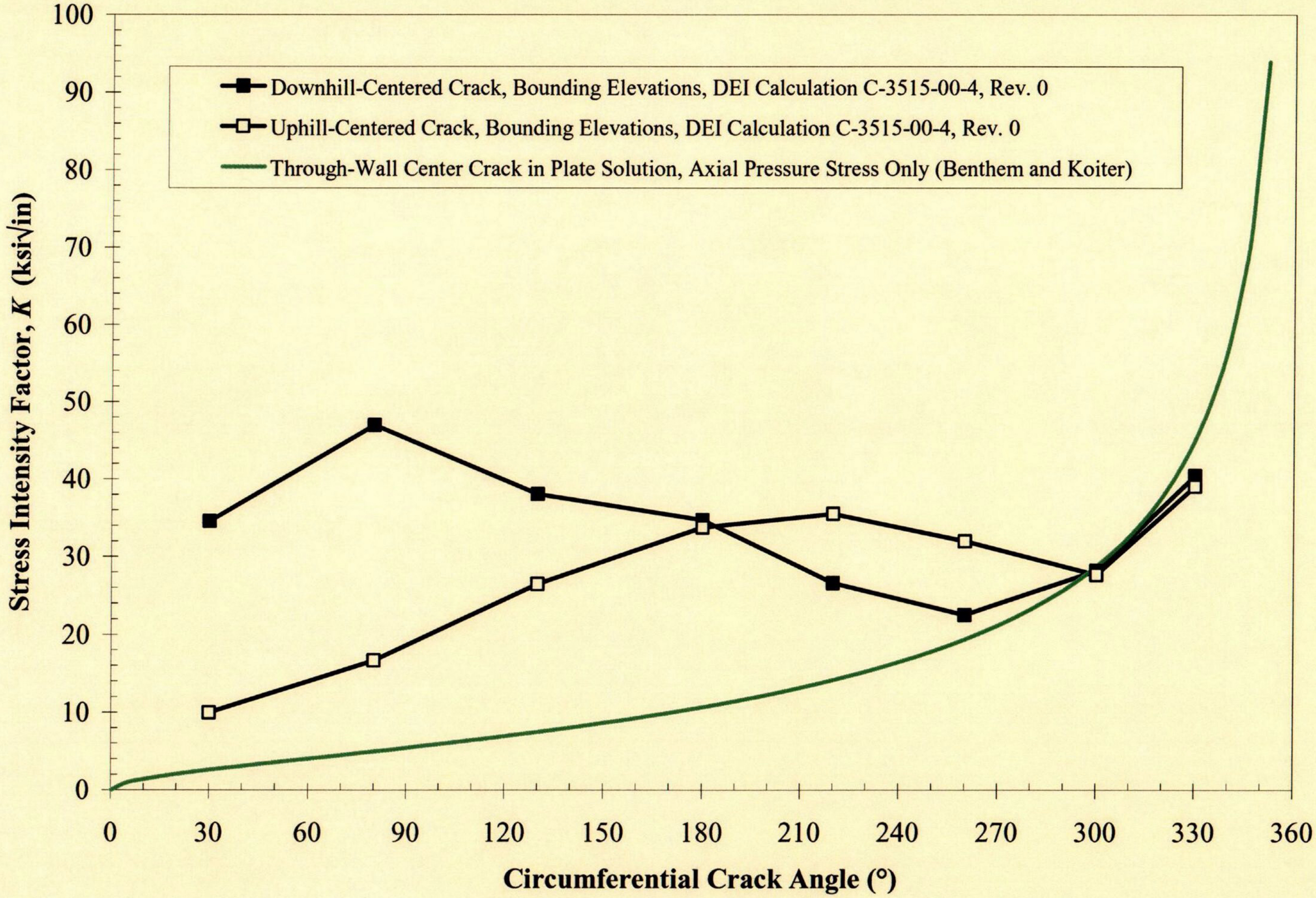

C-09

Effect on Nozzle Ejection Assessments
Improvement in Deterministic Results

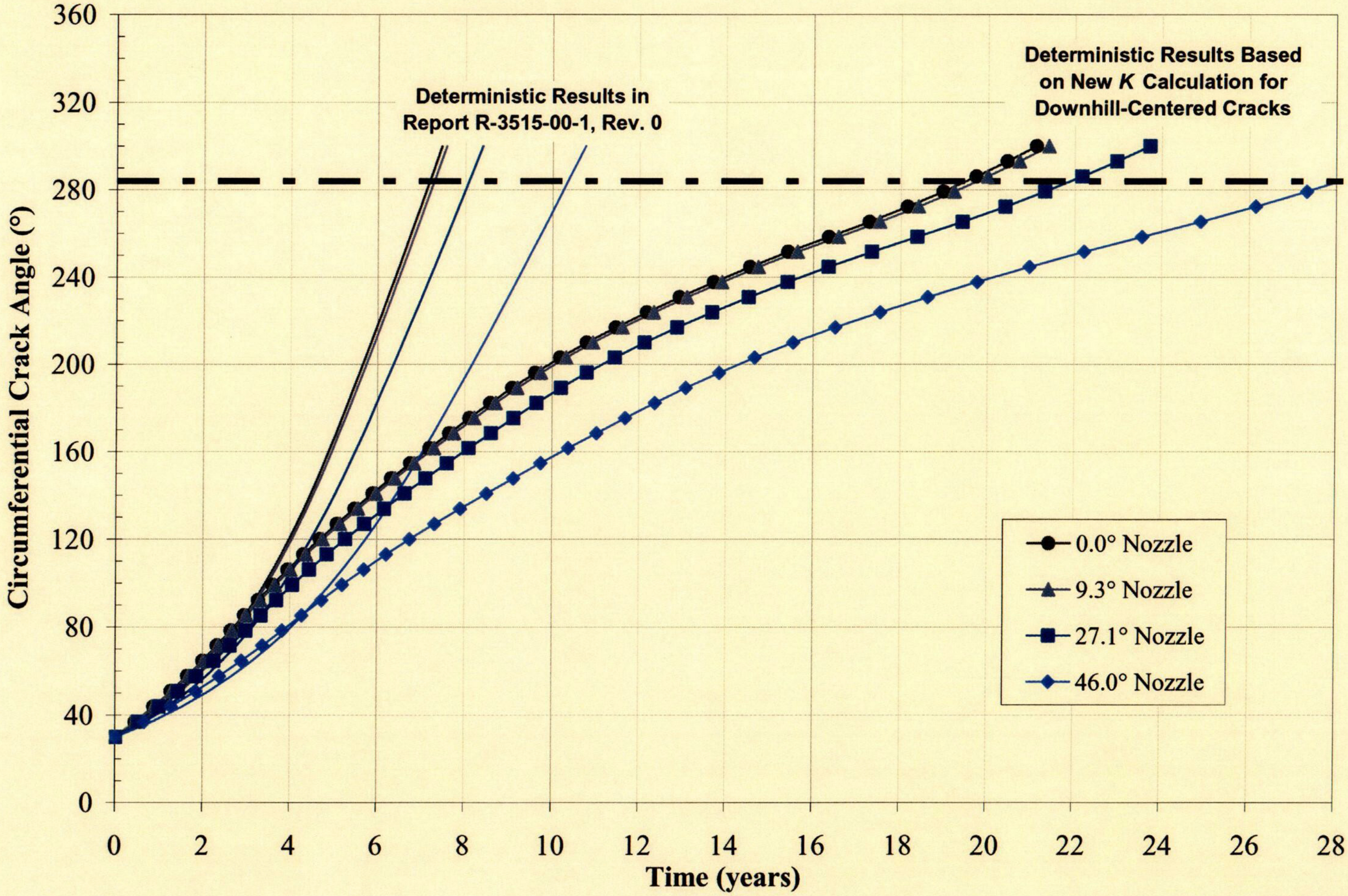

C-10

Effect on Nozzle Ejection Assessments
Improvement in Probabilistic Results

- Probabilistic results for the base case and three sensitivity cases were generated by substituting the new "bounding elevation" stress intensity factor curves calculated for Robinson for the previously assumed curves:

Sensitivity Case per Table 8-6 of Report R-3515-00-1, Rev. 0		Maximum $\Delta CDF_{ejection}$ for RO-21 to RO-23 Evaluation Period (per year)	
No.	Description	R-3515-00-1, Rev. 0, Results	Using New Stress Intensity Factor Curves
0	Base Case	1.0×10^{-7}	1.0×10^{-8}
1	ECT POD: *Multiply POD Curve by 0.8*	8.7×10^{-7}	1.2×10^{-7}
7b	Crack Growth Rate: *Use Top ¼ of Distribution*	8.4×10^{-7}	2.0×10^{-8}
12	ID Craze Indications: *4 nozzles initiate cracks RO-21*	1.4×10^{-6}	1.2×10^{-8}

Effect on Nozzle Ejection Assessments
Conclusions

- The stress intensity factor curve assumed in DEI Report R-3515-00-1, Rev. 0, for downhill-centered circumferential nozzle cracks is conservatively high for the H. B. Robinson plant

- Using a methodology that considers factors such as stress redistribution in the cracked condition, a stress intensity factor in the range of 20 to 50 ksi$\sqrt{in}$ was calculated for the outer row Robinson CRDM nozzle

- The new stress intensity factor results indicate considerable conservatism in the deterministic and probabilistic nozzle ejection assessments presented in DEI Report R-3515-00-1, Rev. 0

H. B. Robinson CRDM Through-Wall Circumferential Crack Fracture Mechanics Analyses

Record of Revisions				
Rev.	Description	Prepared by Date	Checked by Date	Reviewed by Date
0	Original Issue	D. S. Gross 9/23/03	[illegible] 9/23/03	J. E. Broussard 9/23/03

The last revision number to reflect any changes for each section of the calculation is shown in the Table of Contents. The last revision numbers to reflect any changes for tables and figures are shown in the List of Tables and the List of Figures. Changes made in the latest revision, except for Rev. 0 and revisions which change the calculation in its entirety, are indicated by a double line in the right hand margin as shown here.

Table of Contents

List of Tables

List of Figures

1.0 Purpose

The purpose of this calculation is to document the results of finite element fracture mechanics analyses of through-wall circumferential cracking in the outermost CRDM penetration (46.0° nozzle) at H. B. Robinson Unit 2. The analyses calculate the average crack tip stress intensity (K) for through-wall circumferential cracks that are centered at both the uphill and downhill sides of the nozzle and located at varying elevations at and above the top of the J-groove weld. The stress analyses consider the effects of welding residual stresses in the nozzle, as well as the effect of operating temperature and pressure loading.

2.0 Summary of Results

Average crack tip stress intensities were calculated for through-wall circumferential cracks ranging from 30° to 330° (total crack length), centered at the uphill and downhill sides of the nozzle, at elevations ranging from the top of the weld to one-half inch above the top of the weld for the 46.0° nozzle penetration. These cases support the following conclusions:

1. Average and peak crack tip stress intensities for small through-wall circumferential cracks are higher for downhill-centered cracks than for uphill-centered cracks.

2. Average and peak crack tip stress intensities for downhill-centered cracks increase with circumferential extent for small crack lengths, then tend to decrease and level off as cracks increase toward larger total lengths, finally increasing again as the crack approaches the full circumference of the nozzle.

3. Average and peak crack tip stress intensities for uphill-centered cracks increase with circumferential extent for small and moderate size cracks, then level off as cracks increase toward larger total lengths, finally increasing again as the crack approaches the full circumference of the nozzle.

4. For uphill-centered cracks, average and peak crack tip stress intensities for through-wall circumferential cracks are generally highest at the top of the weld elevation, and generally decrease with increasing height above the top of the weld.

5. For downhill-centered cracks, the dependence of crack tip stress intensity on crack elevation is not significant, with similar calculated values at each elevation.

6. Small downhill-centered cracks tend to have a relatively uniform distribution of crack tip stress intensity across the crack front. As the crack gets longer, the distribution becomes less uniform, with a decreased stress intensity at the nozzle OD.

7. Uphill-centered cracks tend to have the highest crack tip stress intensity at the ID of the nozzle for all crack lengths.

8. The calculated average crack tip stress intensity is positive and well above 10 ksi$\sqrt{in}$ at all crack lengths, suggesting continued crack growth.

3.0 Input Requirements

The following values are used in this calculation:

1. The local configuration of the J-groove weld attaching the CRDM nozzle and the RPV head, detailed dimensions of the RPV head and CRDM nozzles, and welding residual stress calculation methodology were taken from DEI calculation C-3515-00-1, Revision 0 (1).

3. Operating temperature and pressure. An operating head temperature of 598 °F and an operating pressure of 2,250 psig were assumed for this calculation, consistent with the values used in DEI calculation C-3515-00-1, Revision 0 (1).

4.0 Assumptions

The following modeling assumptions were used for the work described in this calculation:

1. The nozzle was assumed to be flush with the penetration. No clearance or interference fit was assumed.
2. Two passes of welding were performed for the welding residual stress analysis: an inner pass and an outer pass. The model geometry was designed such that each weld pass is approximately the same volume.
3. Material yield strengths were selected to be the same as used used in DEI calculation C-3515-00-1, Revision 0 (1).
4. The CRDM nozzle penetration geometry is based on nominal as-designed dimensions.
5. Although the welding residual stress analysis is performed using non-linear material strain hardening properties, the model is converted to a fully elastic model for the crack tip stress intensity calculation. This is appropriate since the data for PWSCC crack growth rate are currently provided as a function of the linear elastic fracture mechanics (LEFM) crack tip stress intensity, K.
6. The finite element fracture mechanics analysis provides J-integral values for the modeled crack front, from which K is calculated. In calculating K from J, the inverse of the formula used to calculate J from K_I, based on linear elastic Mode I loading, is used. This provides an estimate of a total "equivalent" K based on contributions from Modes I, II, and III loading, to the extent they exist.
7. The crack front is modeled using a small-radius key hole, rather than collapsed element faces. Test cases were performed to verify and validate this analytical method (3).

8. Operating pressure is applied to the flanks of the crack, but not to the nozzle OD.
9. The circumferential crack is assumed to follow the contour of the J-groove weld, as it progresses around the nozzle from downhill to uphill (or vice versa).
10. No crack plane elevation cases were considered below the top of the weld because the weld is assumed to be intact for this analysis.

5.0 Analysis

5.1 Finite Element Model Description

Both the initial welding residual stress and subsequent fracture mechanics analyses were performed using 180° symmetric 3-D FEA models. The model includes a sector of the alloy steel head with stainless steel cladding on the inside surface, the Alloy 600 nozzle, the Inconel buttering layer in the J-groove weld prep, and the Inconel weld material divided into two "passes" of approximately equal volume. The stainless steel cladding and Inconel buttering layers were included in the model since these materials have significantly different coefficients of thermal conductivity compared to the carbon steel vessel head, and therefore influence the weld cooling process.

For the welding residual stress analysis, both thermal and structural analyses were performed. In the 3-D thermal analysis, eight-node thermal solids (SOLID70) were used. No thermal connection was provided between the nozzle and head penetration, which limits heat transfer between the nozzle and head to conduction through the J-groove region. This assumption was made because the head penetrations are counterbored both at the upper and lower portions of the penetration, and because thermal communication between the surfaces that are nominally in contact was assumed to be poor.

For both the welding residual stress structural analysis and the subsequent fracture mechanics analyses, eight-node 3-D isoparametric solid elements (SOLID45) and contact surface elements (CONTA173/TARGE170 pairs) were used. In the welding residual stress calculations, the SOLID45 elements replaced the SOLID70 elements used for the thermal analysis. Degenerate four- and six-node solid elements were not used in areas of high stress gradient since they can lead to significant errors when used in these regions (2). Higher order elements were not used since they provide no greater accuracy for elastic-plastic analyses than the eight-node solids (2).

In performing the fracture mechanics analyses, the through-wall circumferential cracks in the nozzle are assumed to follow the elevation of the top of the weld around the nozzle (i.e., the crack is not purely circumferential). For reasons specific to the modeling methods used, the crack front is modeled using a small-radius key hole rather than a set of collapsed element faces. Full operating pressure is applied to the entire crack face during the fracture mechanics analyses. A plot of a sample fracture mechanics finite element model is shown in Figure 5-1. A detailed image of the mesh in the crack tip region, showing the crack front with the key hole, is shown in Figure 5-2.

All finite element analyses were performed on an HP J6700 workstation, under the HP-UX 11.0 operating system and ANSYS Revision 5.7, which is maintained in accordance with the provisions for control of software described in Dominion Engineering, Inc.'s QA Manual for Safety-Related Nuclear Work, DEI-002.

5.2 Welding Residual Stress Analysis

The welding residual stress analysis was performed using the file cirse.base, version 2.4.0, which features a number of modifications relative to the model described in Reference (1), which was created and analyzed using the file cirse.base, version 2.1.5. Many of these modifications are improvements in the features available in the model, including the ability to perform the subsequent fracture mechanics analyses. None of the changes to cirse.base affect the assumptions and methodologies used to calculate welding residual stresses.

5.3 Through-Wall Circumferential Crack Fracture Mechanics Analyses

After the completion of the welding residual stress analysis, which includes the effects of hydrotest pressurization, a series of finite element models were generated to calculate crack tip stress intensities for through-wall circumferential cracks at operating conditions in the presence of welding residual stresses. The stresses calculated by the welding residual stress model were interpolated onto the fracture mechanics portion of the model using a quadratic interpolation rule. Cracks of increasing length were analyzed for models with a crack at the top of the weld, as well as at 0.25 and 0.5 inches above the top of the weld. Cracks below the weld were not considered because the weld is assumed to be intact for these analyses. Each of these cases were analyzed for a crack centered at the uphill and downhill planes of the nozzle. A total of eight crack lengths were analyzed for each model variation: 30°, 80°, 130°, 180°, 220°, 260°, 300°,

and 330°. The crack tip stress intensity was evaluated at eight evenly spaced locations through the wall of the nozzle.

Although the welding residual stress model uses non-linear material strain-hardening properties, the structural model is converted to a fully elastic model for the fracture mechanics analyses. This is appropriate since the correlations for PWSCC crack growth rate are currently provided as a function of the stress intensity, K, which presumes linear elastic fracture mechanics (LEFM). Operating temperature and pressure were applied to each model case starting from the post-hydrotest welding residual stress state, including full operating pressure on the entire crack face. Maximum stresses for representative cases were checked to ensure that the stresses did not exceed reasonable levels for elastic material assumptions outside the crack tip region. It is noted that for the fracture mechanics analyses performed in this calculation, the welding residual stresses are applied as secondary stresses, which redistribute in the presence of the crack. Only the operating pressure is applied as a primary load to the model, both at the model wetted surface and on the crack face. This is a more accurate approach to modeling the stress state of the cracked nozzle than methods such as superposition.

Calculation of the J-integral values at each of the eight points along the crack front through the wall of the nozzle was performed using software developed by DEI. Verification and validation of this software is discussed in Reference (3). The software reads the elastic strain at the crack front elements from the ANSYS results file and performs the J value integration calculations using a numeric volume integration routine. As an output, the software reports the J-integral value as a function of distance along the crack face. Using the relationship between J and K described on page 125 of (4) for the special case of linear elastic materials and using plane strain conditions, the crack tip stress intensity is calculated from the J-integral values with the following equation:

$$K = \sqrt{\frac{J \times E}{1 - \nu^2}} \qquad [5\text{-}1]$$

where,

K = crack tip stress intensity (psi$\sqrt{\text{in}}$)
J = calculated J-integral value (psi•in)
E = modulus of elasticity at 600°F = 28.5 x 10^6 psi
ν = Poisson's ratio = 0.29

It is noted that the J-integral value calculated by the software is the combined result of Modes I, II, and III loading. Therefore, the value for K calculated using Equation 5-1 is an "equivalent" K that is higher than the K associated with any individual loading mode.

When an average crack tip stress intensity is desired, the average of the J-integral values is taken for the entire crack front, then the average J is converted to the equivalent crack tip stress intensity using Equation 5-1.

5.3 Analytical Results Summary

The crack tip J-integral was calculated as a function of through-wall depth for the cases described above. From these results, the average through-wall stress intensity and the peak stress intensity were determined. Plots of the average and peak stress intensity as a function of crack length for each crack plane elevation considered are included in Figures 5-3 and 5-4 for downhill-centered cracks and in Figures 5-5 and 5-6 for uphill-centered cracks. The bounding values from each of these four plots as a function of crack length are summarized in Table 5-1 below, and are plotted in Figure 5-7.

Table 5-1. Bounding Crack Tip Stress Intensity, K (ksi√in) vs. Crack Length

Model Case	Crack Total Length							
	30°	80°	130°	180°	220°	260°	300°	330°
Downhill Average K	34.6	47.0	38.1	34.7	26.6	22.5	28.2	40.4
Downhill Peak K	42.2	56.5	47.3	40.5	34.4	32.4	40.3	53.8
Uphill Average K	10.0	16.7	26.5	33.8	35.5	32.0	27.7	39.1
Uphill Peak K	18.5	23.9	35.7	48.0	44.9	39.0	36.4	50.9

Examination of Figures 5-3 and 5-5 show that, for uphill-centered cracks, the average crack tip stress intensity is nearly always highest at the top of the weld, and decreases as the crack plane elevation above the weld increases. Downhill-centered cracks do not show such a clear trend, but have similar stress intensities at every elevation. Figures 5-4 and 5-6 show a similar trend in peak crack tip stress intensity. Additionally, Figures 5-3 and 5-4 demonstrate that downhill-centered cracks tend to have high stress intensities at small crack lengths that decrease and level off with increasing length; whereas Figures 5-5 and

5-6 show uphill-centered cracks have small stress intensities for small cracks that increase and level off with increasing crack length, before increasing sharply for very long cracks as the pressure load concentrates on the remaining ligament.

The through-wall distribution of crack tip stress intensity is plotted in Figures 5-8 and 5-9 for selected crack lengths of downhill and uphill-centered cracks, respectively. Figure 5-8 shows that small downhill-centered cracks tend to have a relatively uniform distribution of stress intensity across the face of the crack. As the crack gets larger, the distribution becomes less uniform, with a lower stress intensity at the OD of the nozzle. Figure 5-9 shows that uphill-centered cracks tend to have the highest stress intensity at the ID of the nozzle, regardless of the crack length.

6.0 References

1. "H.B. Robinson CRDM Stress Analysis," DEI Calculation C-3515-00-1, Revision 0, July 2003 (proprietary).

2. "Modeling and Meshing Guide," ANSYS 5.7 Documentation, ANSYS, Inc.

3. DEI Memo M-3515-00-7, "Commercial Grade Dedication of Software Used for Calculation of Crack Tip Stress Intensities, September 22, 2003 (proprietary).

4. T.L. Anderson, Ph.D., Fracture Mechanics – Fundamentals and Applications, Second Edition, CRC Press, 1995.

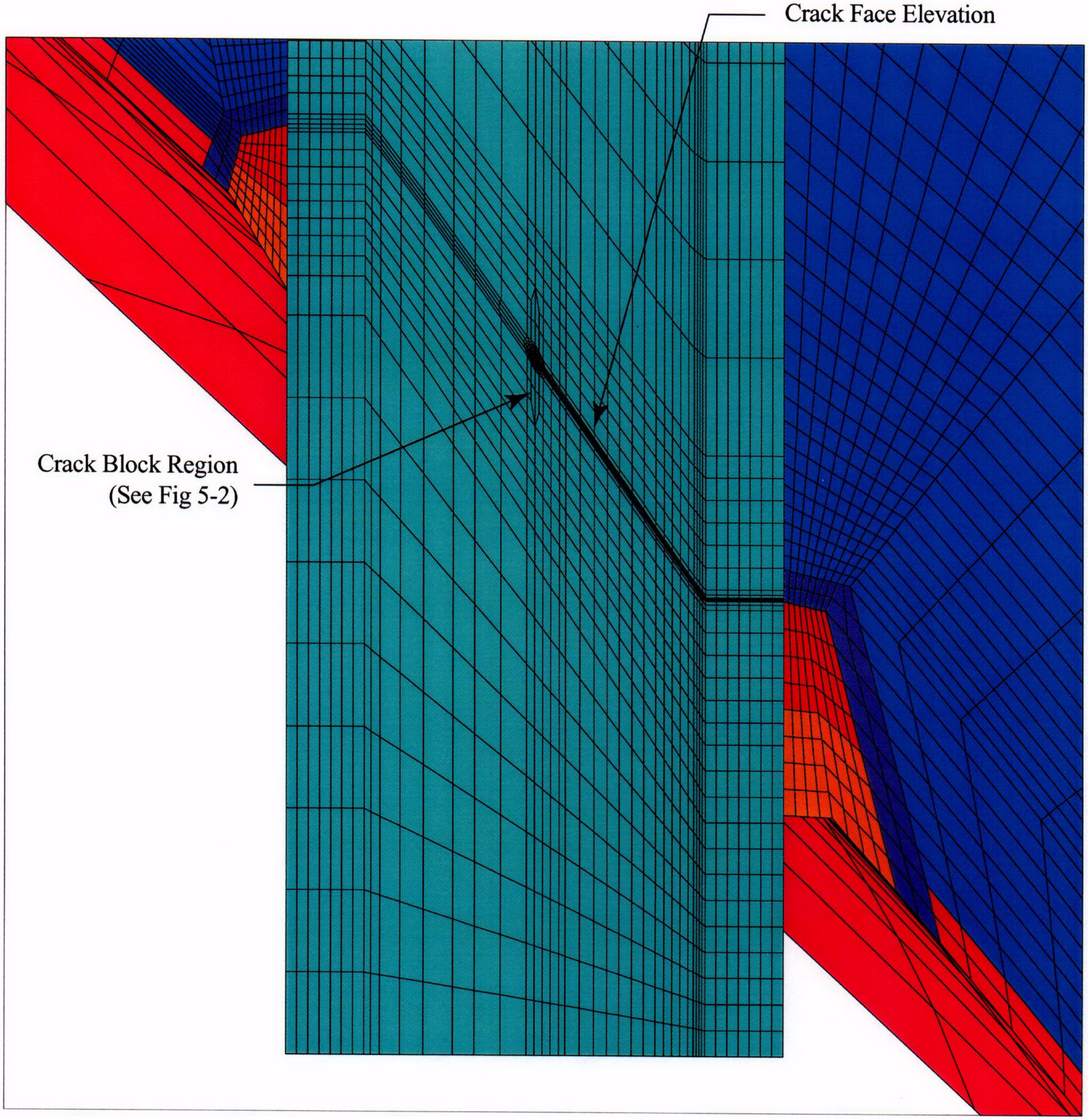

Fracture Mechanics FEA Model (180° Downhill-Centered Crack)

Figure 5-1

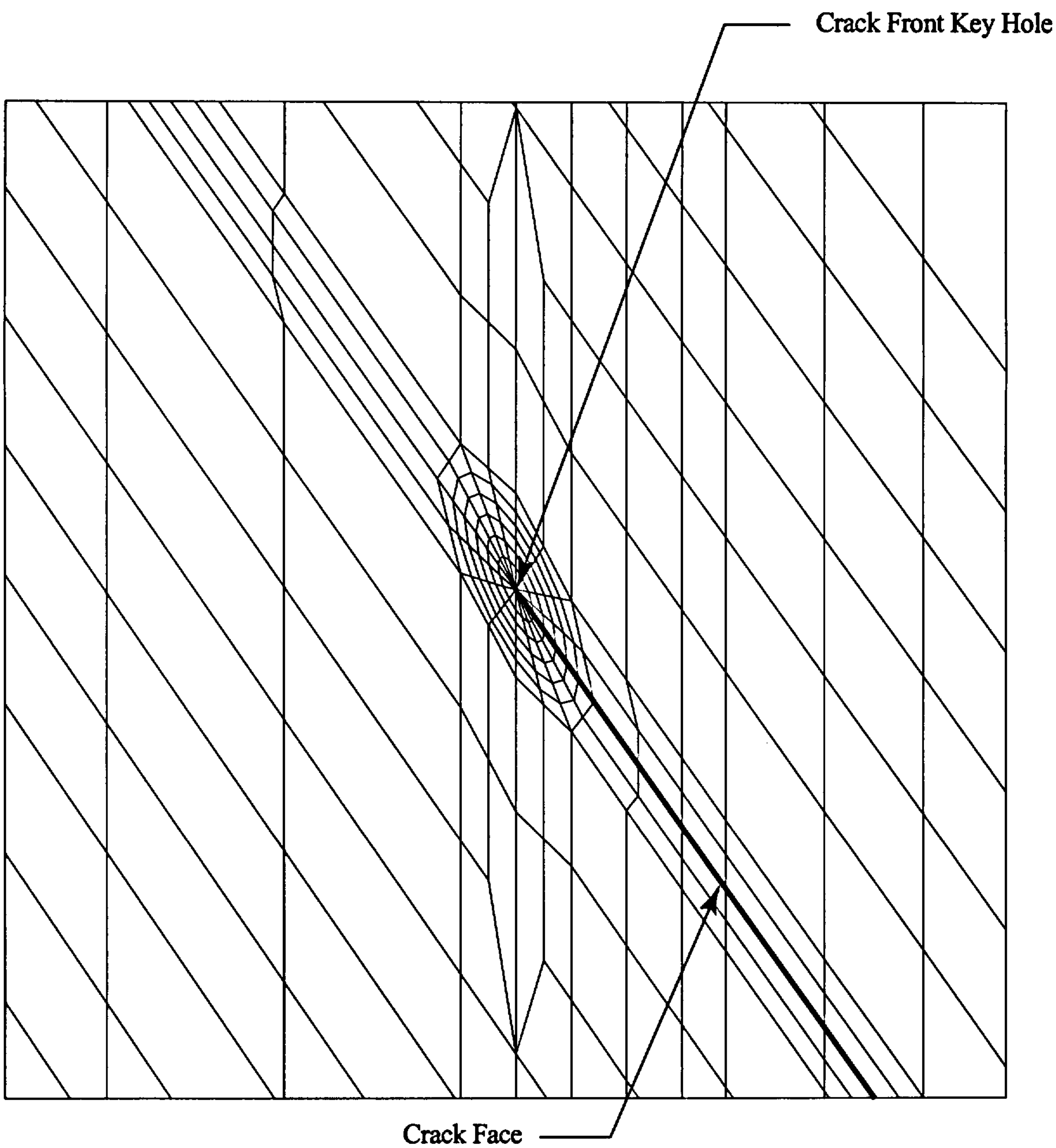

<u>Fracture Mechanics FEA Model (Crack Mesh Detail)</u>

Figure 5-2

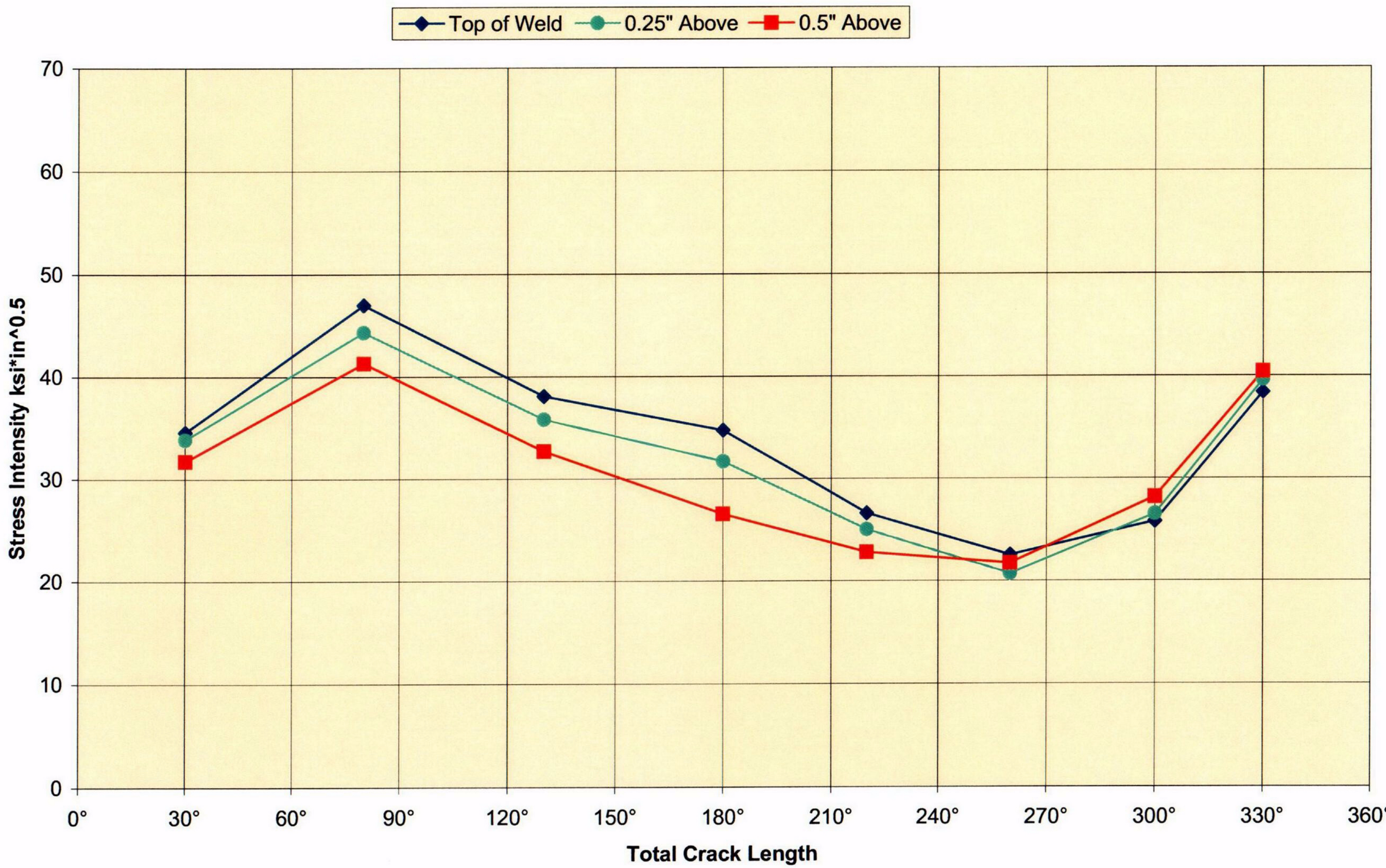

Figure 5-3. Average Crack Tip Stress Intensity For Downhill-Centered Through-Wall Circ Cracks

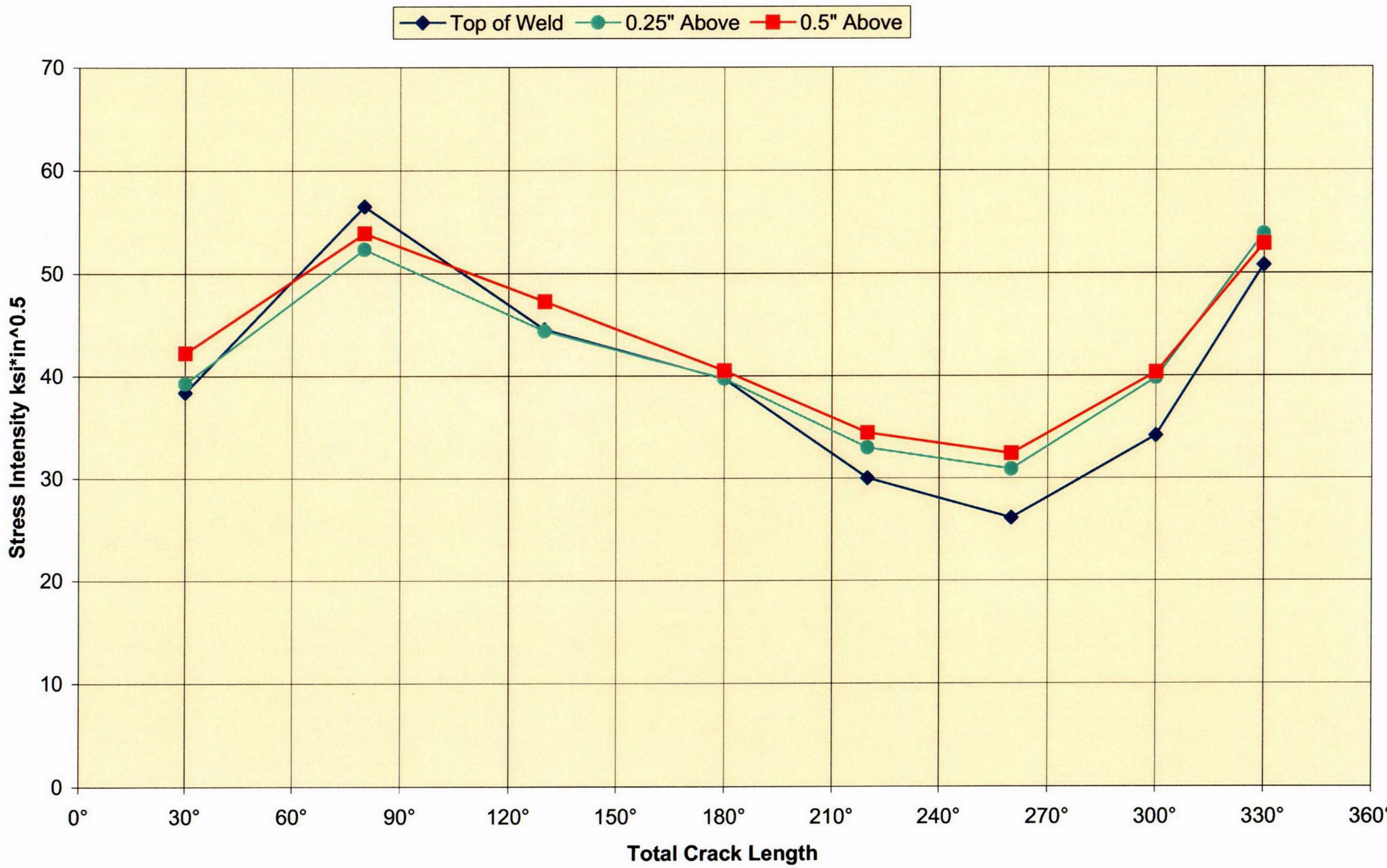

Figure 5-4. Peak Crack Tip Stress Intensity For Downhill-Centered Through-Wall Circ Cracks

C-13

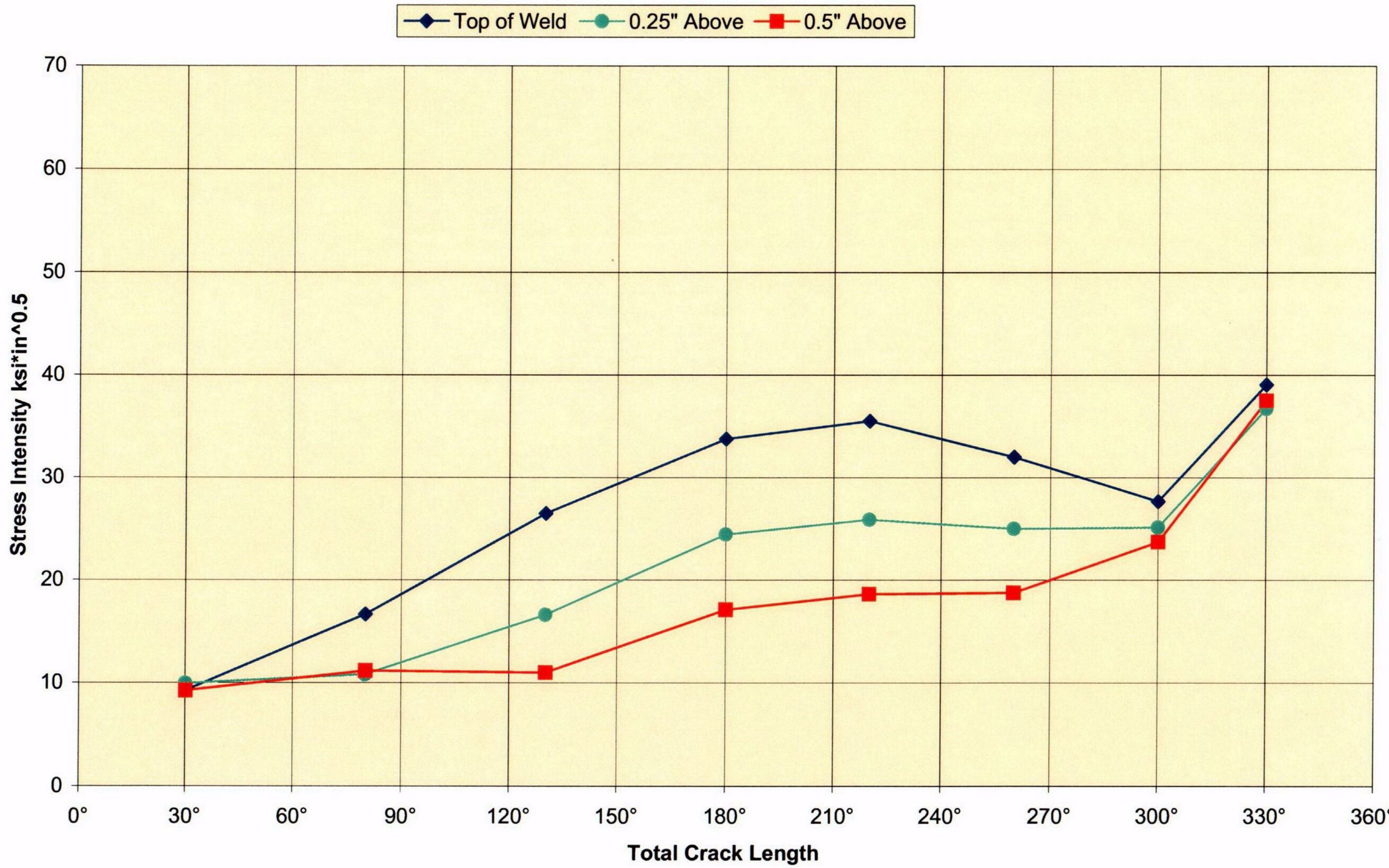

C-14

Figure 5-5. Average Crack Tip Stress Intensity For Uphill-Centered Through-Wall Circ Cracks

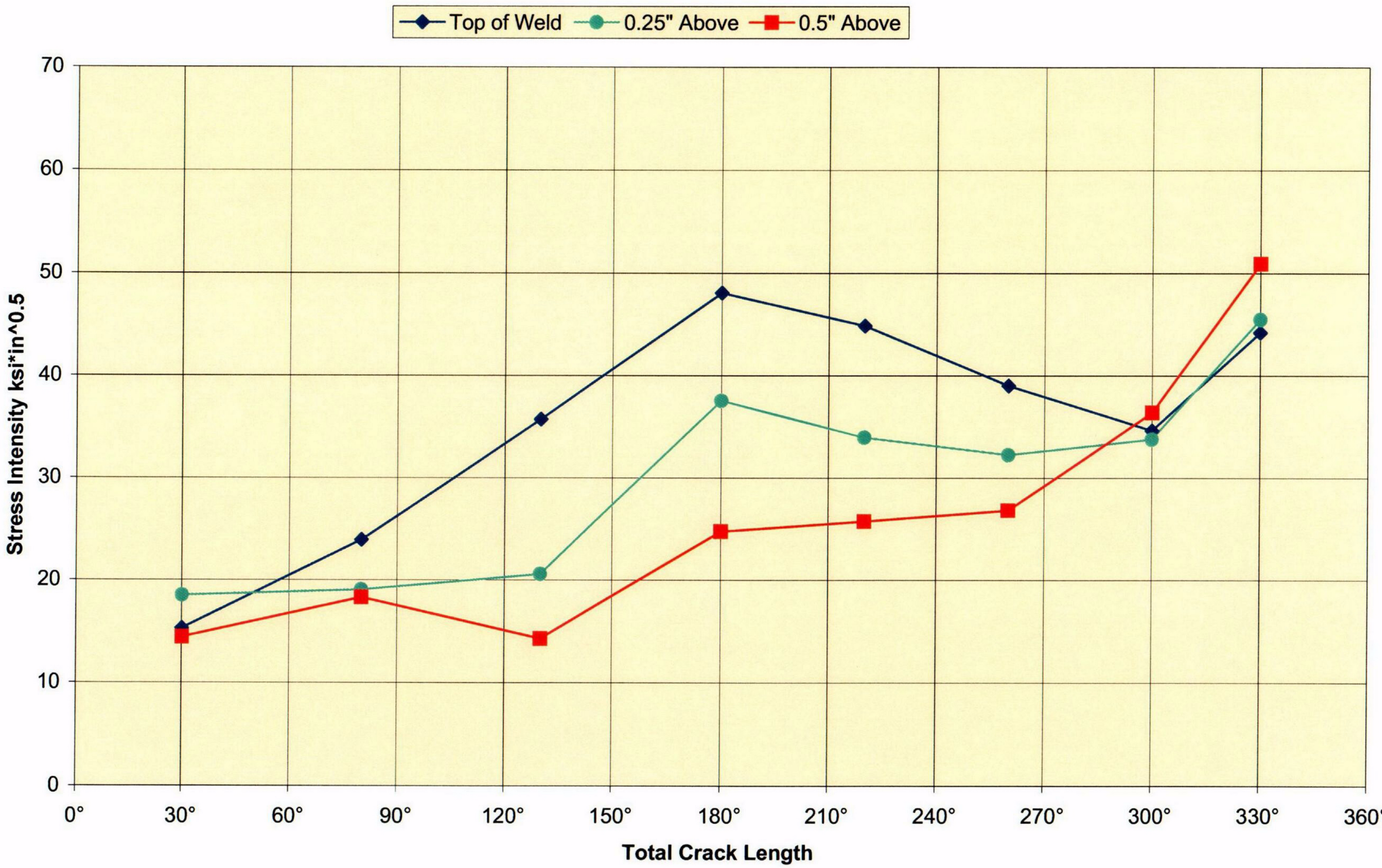

Figure 5-6. Peak Crack Tip Stress Intensity For Uphill-Centered Through-Wall Circ Cracks

C-15

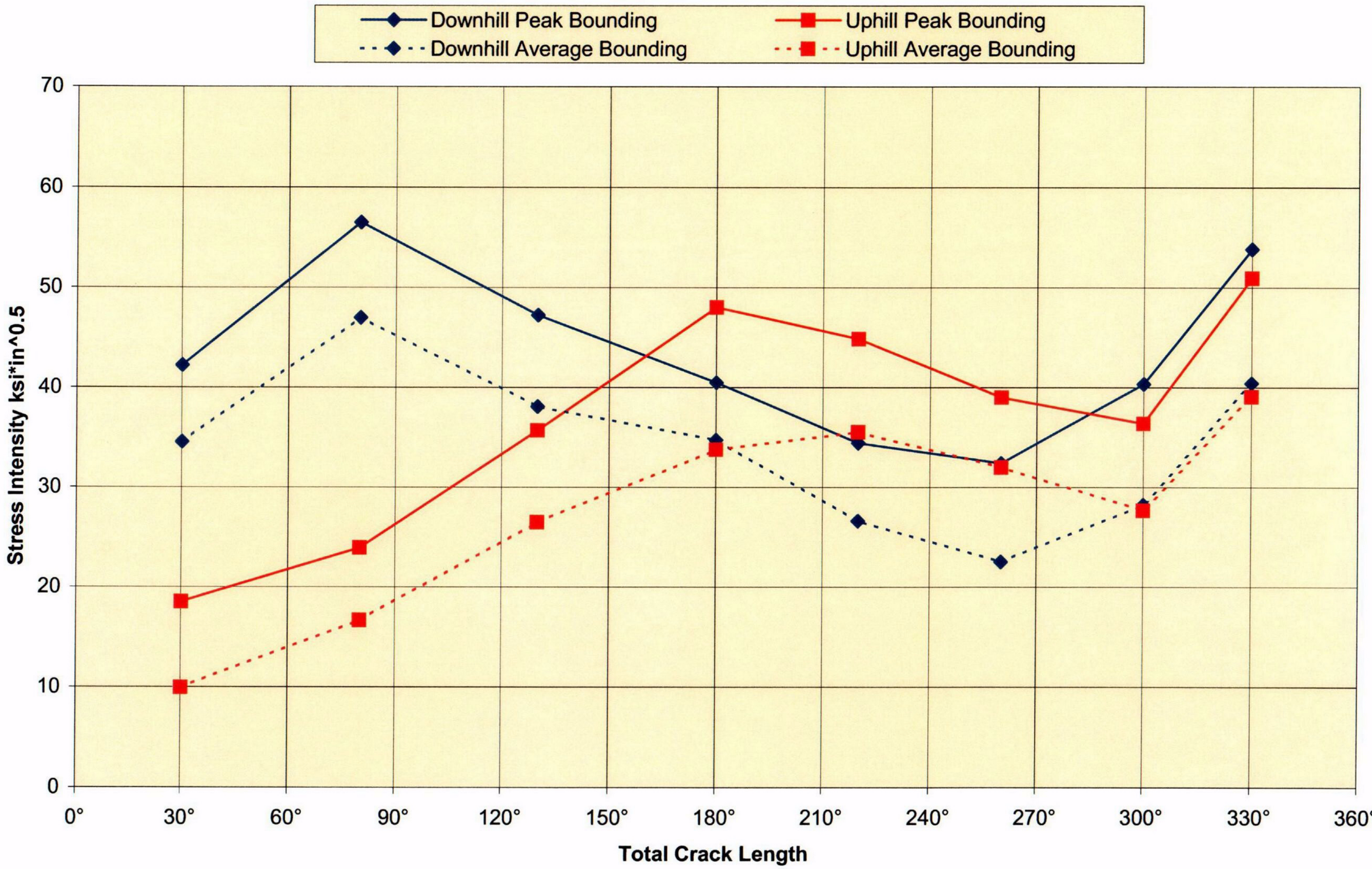

C-16

Figure 5-7. Bounding Crack Tip Stress Intensity For Through-Wall Circ Cracks

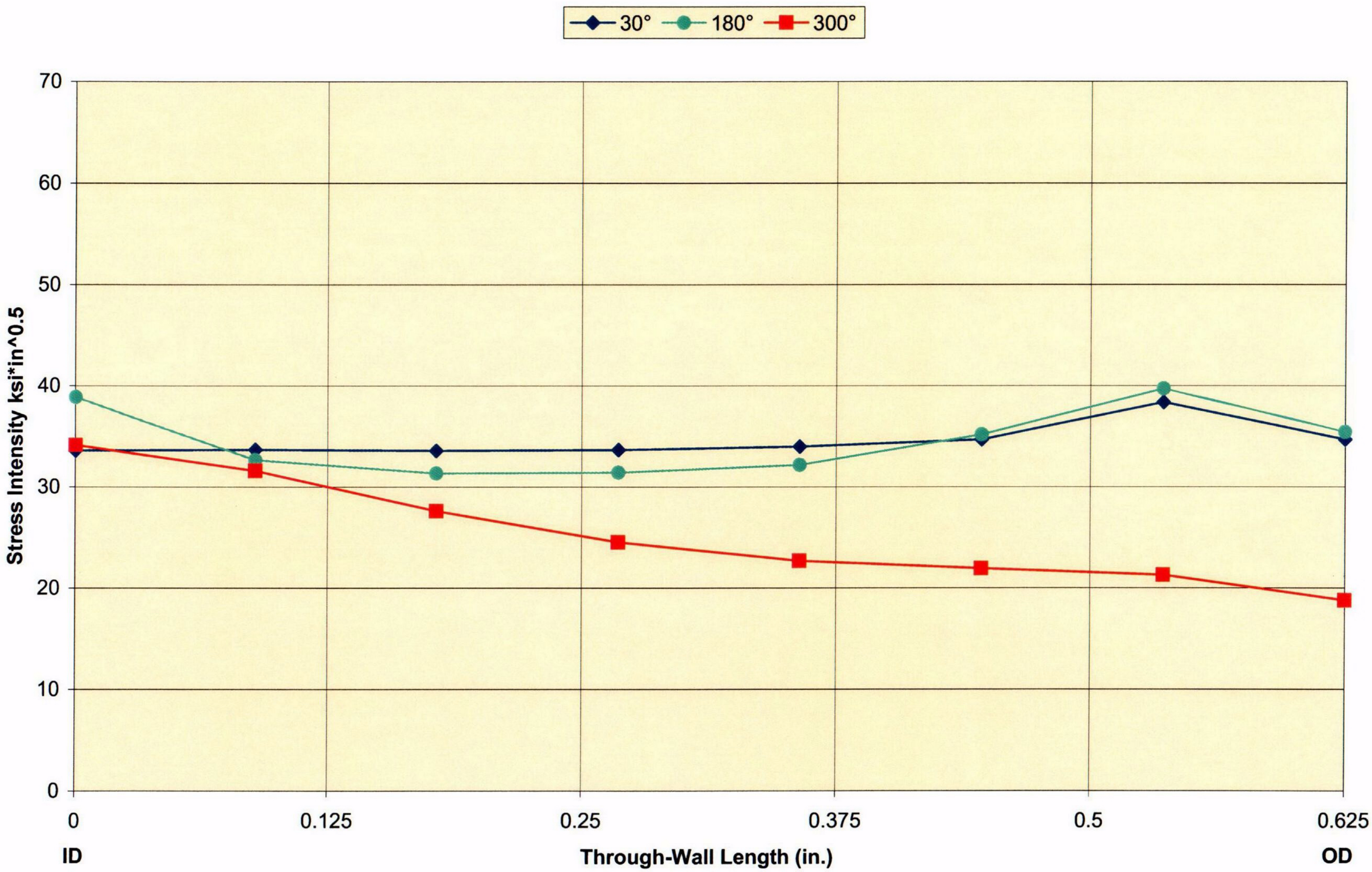

Figure 5-8. Crack Tip Stress Intensity Through-Wall Distribution – Downhill-Centered Crack – Top of the Weld

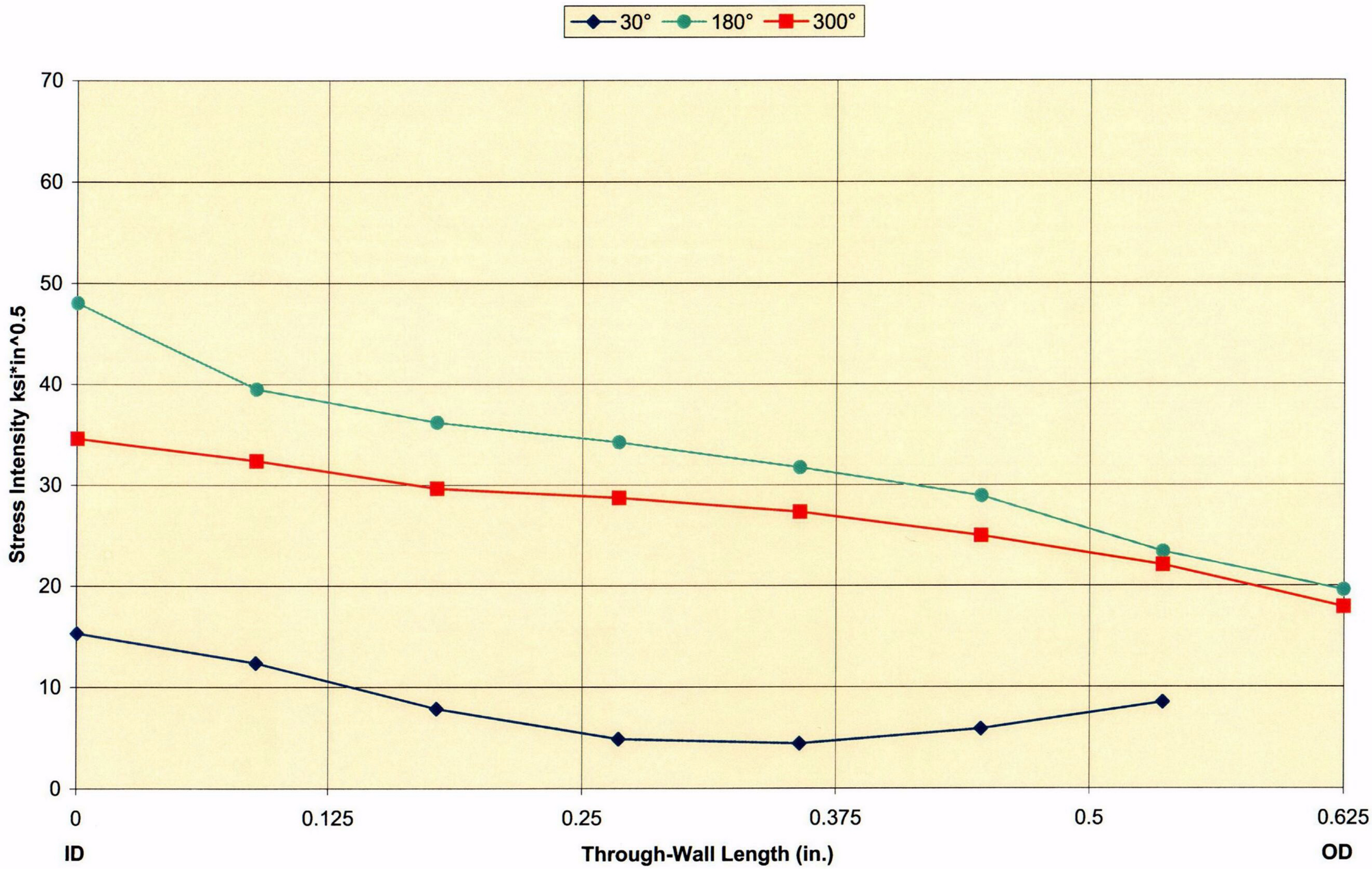

Figure 5-9. Crack Tip Stress Intensity Through-Wall Distribution – Uphill-Centered Crack – Top of the Weld